Pure & Appl. Chem., Vol. 70, No. 4, pp. 917–924, 1998.
Printed in Great Britain.

Iron porphyrins reinvestigated by a new method: Mössbauer spectroscopy using synchrotron radiation

A. X. Trautwein[a], H. Winkler[a], S. Schwendy[a], H. Grünsteudel[a,b], W. Meyer-Klaucke[a], O. Leupold[c], H. D. Rüter[c], E. Gerdau[c], M. Haas[d], E. Realo[d], D. Mandon[e] and R. Weiss[e]

[a] *Physik, Medizinische Universität, 23538 Lübeck, Germany*
[b] *ESRF, BP 220, 38043 Grenoble, France*
[c] *II.Inst. f. Experimentalphysik, Universität Hamburg, 22761 Hamburg, Germany*
[d] *Institute of Physics, Estonian Academy of Science, 2400 Tartu, Estonia*
[e] *Institut Le Bel, Université Louis Pasteur, 67070 Strasbourg, France*

Abstract: Nuclear resonant forward scattering (NFS) of synchrotron radiation represents Mössbauer spectroscopy in the time domain. This new technique complements the conventional nuclear resonance absorption, e.g. Mössbauer spectroscopy in the energy domain, by supplying highly brilliant, polarized, collimated and timed radiation. In NFS the hyperfine interaction of coherently excited nuclei manifests itself as quantum beats, i.e. as modulation of the time-dependent intensity of the transmitted radiation, which is delayed with respect to the incoming synchrotron pulse. We have investigated ^{57}Fe-enriched iron porphyrins to test NFS for first biophysical applications. NFS spectra of the diamagnetic porphyrin $FeO_2(SC_6HF_4)(TP_{piv}P)$ and of the paramagnetic porphyrin $[Fe(CH_3COO)(TP_{piv}P)]^{\cdot}$ were recorded at various temperatures, with and without reference scatterer, with and without applied field . Dynamic molecular properties, e.g. dynamic structural disorder or spin-lattice relaxation document as variation of the time-delayed count rate. Measured NFS spectra were analysed theoretically by programs which are basically the analogue in the time domain compared to the usual calculations in the energy domain.

INTRODUCTION

Nuclear resonant scattering techniques (1), i. e. nuclear forward scattering (NFS) (2-5) and nuclear inelastic scattering (NIS) (6-8), have become available as spectroscopic methods with the 2nd and 3rd generation sources of synchrotron radiation.

In the present contribution we focus on NFS, which represents Mössbauer spectroscopy in the time domain, and which complements the conventional nuclear resonance absorption, e.g. Mössbauer spectroscopy in the energy domain. NFS makes use of the specific properties of synchrotron radiation, e.g. high brilliance (large flux of light within a narrow bandwidth of energy), high degree of polarization, timed structure of radiation (narrow and equidistant pulses of light) and high degree of beam collimation (~ 1 mm^2 at the 3rd generation machines). NFS is used to study hyperfine interactions and, via effective sample thickness, also molecular dynamics. Here we present first biophysical applications, i. e. on the "picket-fence" porphyrins $FeO_2(SC_6HF_4)(TP_{piv}P)$ and $[Fe(CH_3COO)(TP_{piv}P)]^{\cdot}$.

With respect to NIS, which we have employed to study molecular vibrations in an iron(II) spin-crossover complex, we refer to separate contributions which we present at this conference (9) and at the International Conference on the Applications of the Mössbauer Effect (ICAME 97) (10).

EXPERIMENTAL

The time dependence of NFS intensity was obtained with the nuclear resonance station at beamline BW4 (11) of HASYLAB, DESY in Hamburg, Germany (Fig. 1). The beam of white X-rays was monochromatized by a double-crystal Si(111) premonochromator to a bandwidth of about 2.5 eV at the resonance ener-

gy of 14.413 keV for ^{57}Fe. A further decrease of bandwidth down to 6.5 meV was obtained with a "nested" high-resolution monochromator (12, 13). This beam was used to coherently excite the 14.413 keV nuclear level of ^{57}Fe nuclei in the sample. The sample was mounted in a cryostat to allow measurements at different temperatures and in applied magnetic fields.

When the synchrotron beam of ~ 150 ps length hits the sample electronic X-ray scattering occurs instantaneously while the nuclear scattering process, involving coherent collective nuclear excitation (nuclear exciton) and deexcitation, is only completed after same delay. Note that the mean life time of the first excited state of a single ^{57}Fe nucleus is τ = 141 ns. This property allows to separate the prompt electronic-scattering signal from the nuclear-scattering signal. The latter appears after the nuclear decay as time-delayed coherent electromagnetic radiation which is counted by a fast avalanche photo diode (14).

NFS SPECTRA VERSUS CONVENTIONAL MÖSSBAUER SPECTRA

The time dependence of the intensity of the delayed radiation for the special case of electric quadrupole interaction is given by (15):

$$I(t) \sim e^{-t/\tau} \cos^2\left(\frac{\Delta E_Q \cdot t}{2\hbar}\right). \quad (1)$$

Eq. (1) documents that a conventional single-line Mössbauer spectrum (with zero quadrupole splitting, $\Delta E_Q = 0$, and natural line width) exhibits as exponential with the time dependence of the nuclear decay $e^{-t/\tau}$ (Fig. 2a), while a quadrupole splitting $\Delta E_Q = \hbar 2\pi/T$ exhibits as quantum-beat spectrum with period T superimposed over the exponential $e^{-t/\tau}$ (Fig. 2b).

In case of magnetic hyperfine splitting beating occurs among several resonance lines with the result that the beat pattern becomes more complicated than that shown in Fig. 2b (see below).

Another important feature of coherent scattering by an ensemble of nuclei is the speed-up of the nuclear decay and the modulation of the time evolution due to multiple scattering (4). On account of this effect the time dependence of the intensity of the delayed radiation becomes dependent on the effective sample thickness, t_{eff} (16):

$$I(t_{eff}, t) \sim e^{-t/\tau}\, t_{eff}^2 \left(\frac{J_1\left(\sqrt{t_{eff}\, t/\tau}\right)}{\sqrt{t_{eff}\, t/\tau}}\right)^2. \quad (2)$$

This results in dynamical beats which have in contrast to quantum beats no constant frequency, but the distance of the beats increases with time. The minima of the dynamical beats may be used to determine t_{eff} and from this the Lamb-Mössbauer factor f_{LM} .

Eq. (1) applies for "thin" nuclear scatterers, e. g. for effective thickness of $t_{eff} < 1$. Using a cylindrical sample with a volume of 0.5 ml and a basal area of 0.5 cm^2 the situation $t_{eff} \sim 1$ corresponds to a concentration of about 1 mM in ^{57}Fe (yielding a quadrupole doublet with ~ 10 % resonance effect in the energy domain). Samples with higher concentration, i. e. with higher effective thickness, $t_{eff} > 1$, exhibit additionally to the quantum beats the modulation of the forward scattering intensity (dynamical beats) according to eq. (2) (Fig. 2c).

APPLICATIONS

Diamagnetic "picket-fence" porphyrin $FeO_2(SC_6HF_4)(TP_{piv}P)$

A powder sample of the ^{57}Fe-enriched "picket-fence" porphyrin $FeO_2(SC_6HF_4)(TP_{piv}P)$ was our first test object for biophysical NFS applications. We have used a powder sample instead of a frozen solution to

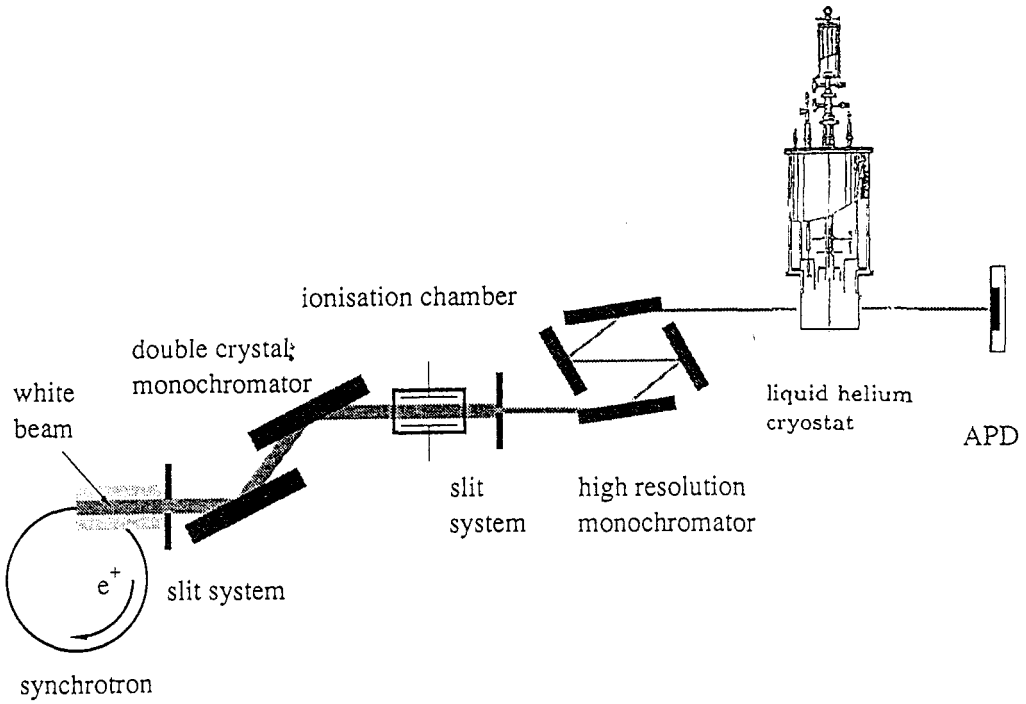

Fig. 1 NFS beamline BW4 at HASYLAB, DESY, Hamburg. The "white" X-rays are monochromatized in two successive steps, i.e. by a double crystal high-heat-load premonochromator and by a high-resolution monochromator, to a bandwidth of ~ 6.5 meV at the resonance energy of 14.413 keV for ^{57}Fe. The liquid helium cryostat with two superconducting split pairs in orthogonal setting allows to investigate samples in the temperature range 2.7 to 300 K, and in applied fields up to 7 T (in various directions relative to the synchrotron beam). As fast detector serves an avalanche photo diode (APD) with a time resolution of ~ 1 ns capable for detecting up to ~ 10^8 photons per second.

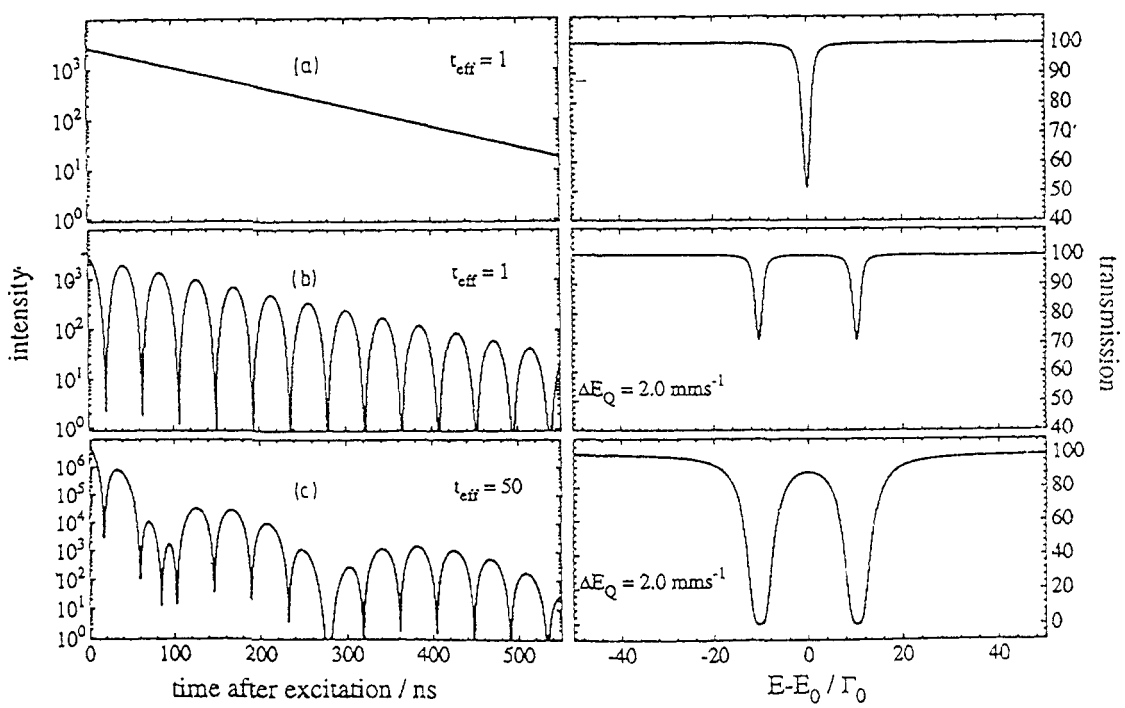

Fig. 2 Mössbauer spectra in the time domain (left) and in the energy domain (right). Note that the isomer shift of a sample does not influence the time evolution of the NFS spectra. Spectra were generated by the CONUSS program (17).

obtain high effective thickness, i.e. to produce spectra with reasonable statistics in times as short as possible. With the small forward scattering count rates R between 12 and 3.5 Hz the NFS spectra with the simple beat pattern arising from a quadrupole splitting (Fig. 3) took between 1 and 3 hours, depending on R. Recording more complicated magnetic spectra took up to 10 hours. A disadvantage of using powder samples, however, is that they are inhomogeneous compared to solutions, which yields a spread of dynamical beat minima and therefore requires additional parameters in the fit analysis (18).

We have measured NFS spectra of two different samples of $FeO_2(SC_6HF_4)(TP_{piv}P)$ at various temperatures, with some of them shown in Fig. 3. From one sample we have also recorded spectra in applied fields of 4 T pointing into different directions within a plane which is perpendicular to the synchrotron beam (Fig. 4). All spectra were analyzed with the CONUSS program (17), assuming that the inhomogeneity within the powder samples is represented by a rectangular thickness distribution, t_{eff} (1±0.25). The porphyrin $FeO_2(SC_6HF_4)(TP_{piv}P)$ is diamagnetic therefore the only magnetic contribution in the analysis of the spectra shown in Fig. 4 is the applied field. We have implemented the field rotation here to test the cryomagnet system (Oxford Instruments), which was specially designed for NFS applications in particular of paramagnetic systems, and also to test the fitting of NFS spectra under various conditions. The CONUSS fits of the NFS spectra in Fig. 3 and 4 are of about the same quality with mean square error deviations (χ^2) around 2.

Note that the NFS spectra in Fig. 3 and in Fig. 4 are not influenced by the isomer shift, δ. In order to determine δ preferably a single-line reference scatterer (e.g. stainless steel or $K_4(Fe(CN)_6)$ has to be placed, additional to the investigated sample, into the synchrotron beam, either up- or down-stream of the cryostat. With this experimental setup beating occurs between three lines, e.g. the single-line from the reference scatterer and the two quadrupole lines from $FeO_2(SC_6HF_4)(TP_{piv}P)$. A fit of the corresponding NFS spectrum (Fig. 5) with the CONUSS program (17) yields an isomer shift of the porphyrin relative to stainless steel of $\delta = 0.30$ mms^{-1}.

In Fig. 6 we have plotted the obtained temperature dependence of the quadrupole splitting ΔE_Q, which compares well with the results from Mössbauer spectra in the energy domain (19). We have originally attributed this temperature variation of ΔE_Q to the dynamic distribution of one of the two oxygen atoms in $FeO_2(SC_6HF_4)(TP_{piv}P)$, which causes a time - and temperature-dependent electric field gradient (efg) tensor at the ^{57}Fe nucleus (18). This view is now additionally suported by the NFS study, which provides new access to dynamic processes in molecules. The obtained effective thickness, t_{eff}, of $FeO_2(SC_6HF_4)(TP_{piv}P)$ (Fig. 7) is a measure of the number of ^{57}Fe nuclei which take part in the coherent collective excitation. The dynamic distribution of the oxygen atom represents in fact the stochastic fluctuation of the efg tensor which destroys the coherence between the excited nuclei. The resulting dephasing reduces the probability for the excitation of the nuclear exciton. As a consequence the forward scattered intensity is reduced, which formally exhibits as reduction of t_{eff} compared to the static situation at low temperature. At elevated temperatures, when the fluctuation rates get much faster compared to the quadrupole precession frequency, certain components of the efg tensor cancel to zero, and the remaining components are constant, independent of a further increase of temperature; hence, the coherence between the excited nuclei is retained and t_{eff} follows the normal trend with increasing temperature.

A similar behavior of the temperature variation of the intensity of delayed counts has been observed in the NFS study of other molecular systems which exhibit dynamic properties: both, the spin-lattice relaxation in the paramagnetic "picket-fence" porphyrin $[Fe(CH_3COO)(TP_{piv}P)]^-$ and the superparamagnetic relaxation in ferritin are accompanied by a minimum of delayed count rate in the intermediate relaxation regime where the stochastic fluctuations of the spin systems destroy the coherence between the excited nuclei (20).

Paramagnetic "picket-fence" porphyrin $[Fe(CH_3COO)(TP_{piv}P)]^-$

For a thick sample, which consists of randomly oriented diamagnetic ^{57}Fe-containing molecules in an applied field, the response of this sample on the incident monochromatized and fully polarized synchrotron beam has been given analytically, e.g. in the CONUSS program (17). This, however, is not possible in the general case of having randomly oriented paramagnetic instead of diamagnetic ^{57}Fe-containing

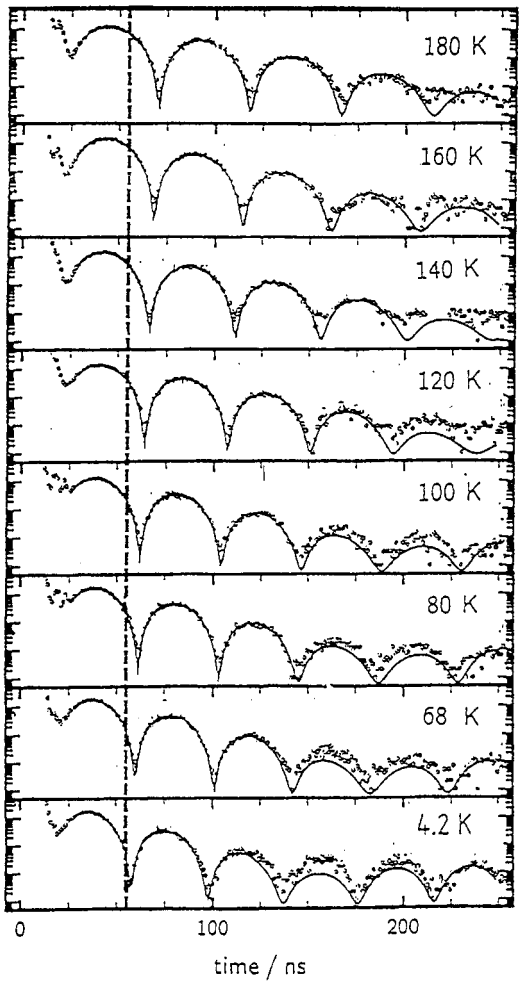

Fig. 3 Experimental NFS spectra of $FeO_2(SC_6\ HF_4)(TP_{piv}P)$ recorded at various temperatures as indicated. The solid lines are fits obtained with the CONUSS program (17). The resulting quadrupole splitting ΔE_Q and effective thickness t_{eff} is plotted versus temperature in Fig. 6 and Fig. 7.

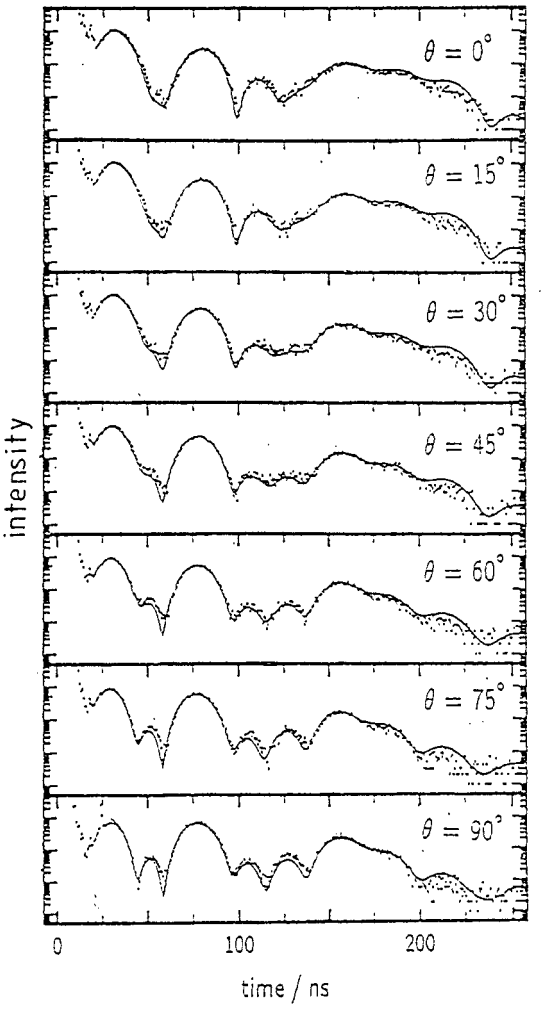

Fig. 4 Experimental NFS spectra of $FeO_2(SC_6\ HF_4)(TP_{piv}P)$ recorded at 4.2 K in a field of 4 T, applied at different angles Θ within a plane which is perpendicular to the synchrotron beam. Θ = 0 represents a field orientation parallel to the polarization $\bar{\sigma}$ of the beam. The solid lines are fits with the CONUSS program (17).

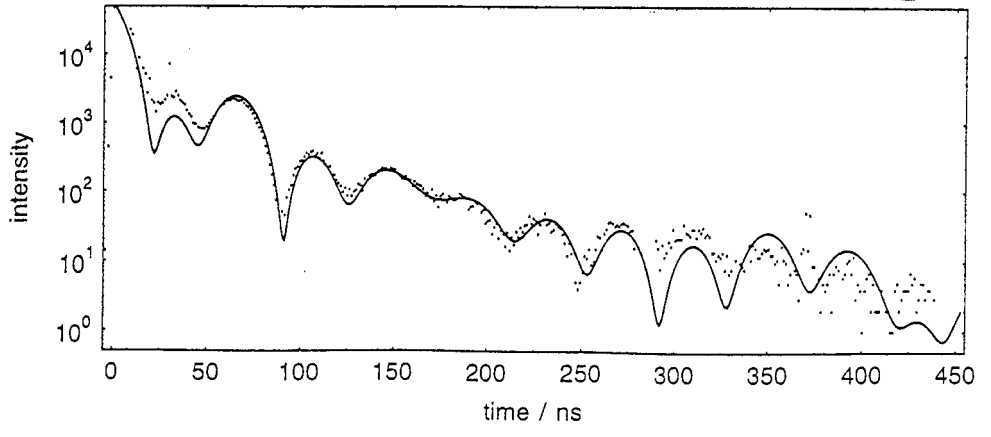

Fig. 5 Experimental NFS spectrum of $FeO_2(SC_6HF_4)(TP_{piv}P)$ at 4.2 K together with stainless steel at 300 K as reference scatterer, the latter placed ~ 30 cm downstream and outside the cryostat. A fit with the CONUSS program (17) yields as isomer shift of the porphyrin relative to stainless steel the value $\delta = 0.30$ mms^{-1}.

molecules in an applied field, because of the integrations involved. The way how to evaluate NFS spectra for this general case numerically by the SYNFOS program has been outlined elsewhere (21). Here we present as first test case measured and calculated NFS spectra of a powder sample of the paramagnetic "picket-fence" porphyrin [Fe (CH_3COO)($TP_{piv}P$)]$^-$ in applied fields.

Application of a field $\vec{B}$ to a ferrous high-spin complex induces spin-expectation values according to the spin-Hamiltonian (22)

$$H = \hat{\vec{S}} \cdot \tilde{D} \cdot \hat{\vec{S}} + \beta_e \, \hat{\vec{S}} \cdot \tilde{g} \cdot \vec{B}. \qquad (3)$$

$\tilde{D}$ and $\tilde{g}$ are tensors describing electronic spin-orbital and Zeeman interaction, respectively, $\hat{\vec{S}}$ represents the effective spin operator, and β_e is the Bohr magneton. The spin-expectation values depend on the orientation of the applied field with respect to the molecular frame of reference. Accordingly, the magnetic hyperfine splitting of the nuclear levels is characterized for the randomly oriented paramagnetic sample by a complicated band of resonant absorptions. The specificity of this band in the present case is defined by the spin-Hamiltonian parameters of [Fe(CH_3COO)(TPpivP)]$^-$, which are D = -0.8 cm^{-1}, E/D = 0 for the zero-field splitting and $A_{x,y}/g_n\beta_n$ = -17 T, $A_z/g_n\beta_n$ = -12 T for the magnetic hyperfine coupling parameters (23) with g_n and β_n representing the nuclear g-factor and the nuclear magneton. Fig. 8 gives the results of SYNFOS calculations for these parameters, with temperature T = 4.2 K and field B = 6 T applied perpendicular to the wave vector $\vec{\kappa}$ and to the polarization $\vec{\sigma}$ of the synchrotron beam. The calculated NFS spectra for ΔE_Q = 4.25 mms^{-1}, η = 0 and 0.2 demonstrate the sensitivity of the forward scattering intensity on the asymmetry parameter η, compared to Mössbauer spectra in the energy domain. Similar sensitivity is achieved for other parameters, provided the NFS measurements are performed to high enough delay times.

In Fig. 9 experimental NFS spectra of [Fe(CH_3COO)(TPpivP)]$^-$ are shown, which were recorded at 3.3 K in an external field of 6.0 T applied (a) perpendicular to $\vec{\kappa}$ and $\vec{\sigma}$ and (b) perpendicular to $\vec{\kappa}$ and parallel to $\vec{\sigma}$ of the incoming beam. The sample had very high effective thickness (t_{eff}) in order to guarantee reasonable statistics at least up to a delay time of ~ 150 ns. Any distribution in t_{eff}, which very likely occurs in a thick powder sample, would affect the dynamical beat structure of the NFS spectra. The solid lines in Fig. 9 represent SYNFOS simulations with the parameters from above and with t_{eff} = 20. Even without the further improvement due to a thickness distribution the calculations reflect the main features of the measured NFS spectra.

In an actual attempt to unambiguously derive Mössbauer and spin-Hamiltonian parameters from a SYNFOS analysis of experimental NFS spectra a number of different experimental conditions (temperature, magnitude and direction of applied field) have to be met. In this respect Mössbauer spectroscopy in the energy domain and in the time domain are comparable.

CONCLUSION

The first biophysical applications of nuclear resonant forward scattering presented here demonstrate the usefulness of ^{57}Fe-Mössbauer spectroscopy with synchrotron radiation in biology and chemistry. The advantages (i) - (iii) of the time-domain (NFS) versus the energy-domain spectroscopy
(i) high sensitivity of quantum-beat structure on Mössbauer and spin-Hamiltonian parameters, especially when the delayed count rate is detected over several 100 ns,
(ii) high degree of collimation of the synchrotron beam at the 3rd generation machines (beam cross section ~ 1 mm^2 at the European Synchrotron Radiation Facility in Grenoble, allowing small sample volumes of < 50 µl) and
(iii) time structure and polarization of the radiation
are inviting to design experiments which were otherwise not possible.

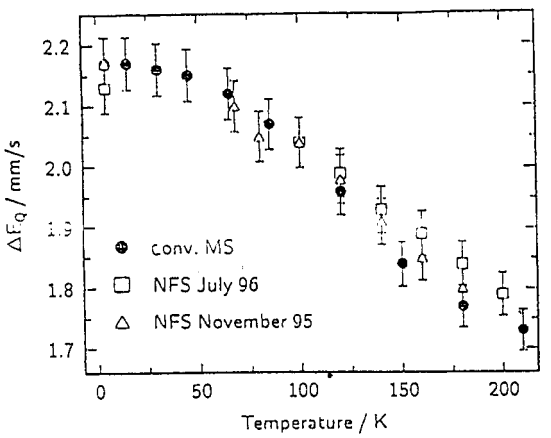

Fig. 6 Temperature dependence of the quadrupole splitting ΔE_Q of $FeO_2(SC_6HF_4)(TP_{piv}P)$ as obtained by NFS and by conventional Mössbauer measurements.

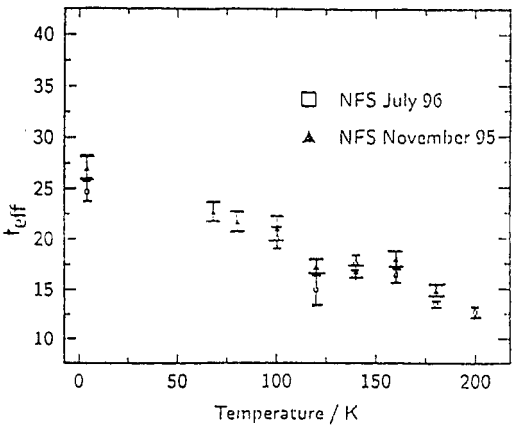

Fig. 7 Temperature dependence of t_{eff} within the rectangular thickness distribution from $0.75t_{eff}$ to $1.25t_{eff}$ of $FeO_2(SC_6HF_4)(TP_{piv}P)$.

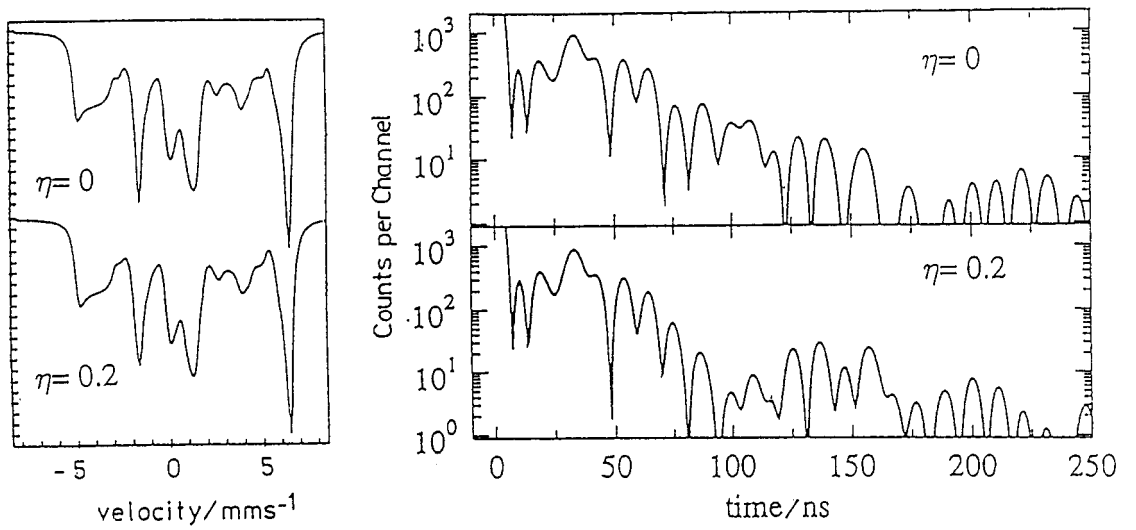

Fig. 8 Mössbauer spectra in the energy domain and in the time domain, calculated with the spin-Hamiltonian parameters of the ferrous high-spin iron porphyrin $[Fe(CH_3COO)(TPpivP)]^-$ (23) for temperature 4.2 K, slow relaxation and applied field of 6.0 T perpendicular to $\vec{\kappa}$ and $\vec{\sigma}$ of the synchrotron beam. The energy-domain spectra were calculated according to the procedure described in (23), and the time-domain spectra result from the new program package SYNFOS described in (21).

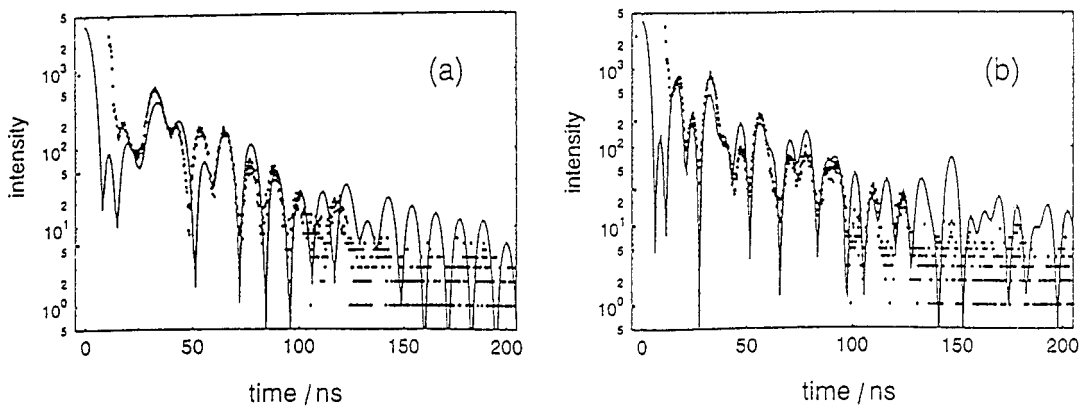

Fig. 9 Experimental NFS spectra of $[Fe(CH_3COO)(TPpivP)]^-$ at 3.3 K in a field of 6.0 T applied (a) perpendicular to $\vec{\kappa}$ and $\vec{\sigma}$ and (b) perpendicular to $\vec{\kappa}$ and parallel to $\vec{\sigma}$ of the incoming beam. The solid lines are calculations with the SYNFOS program using $\eta = 0$ and the spin-Hamiltonian parameters given in the text.

On the other hand, however, the analysis of NFS spectra by simple viewing is restricted to samples which have small effective thickness and which exhibit a single beat frequency only. Otherwise a numerical analysis of the spectra is inevitable.

ACKNOWLEDGEMENTS

The collaborative work reported here was supported by the German Research Foundation (DFG), the German Federal Ministry for Education, Science, Research and Technology (BMBF) and also by the Alexander-von-Humboldt Foundation.

REFERENCES

1. E. Gerdau and U. van Bürck, In: *Resonant Anomalous X-ray Scattering, Theory and Applications*, p. 589. G. Materlik, C. J. Sparks and K. Fischer (Eds.). Elsevier , N. Y. (1994).
2. G. V. Smirnov. *Hyp. Int.* **97/98**, 551 (1996).
3. J. B. Hastings, D. P. Siddons, U. van Bürck, R. Hollatz and U. Bergmann. *Phys. Rev. Lett.* **66 (6)**, 770 (1991).
4. U. van Bürck, D. P. Siddons, J. B. Hastings, U. Bergmann and R. Hollatz. *Phys. Rev.* **B46**, 6207 (1992).
5. U. Bergmann, D. S. Shastri, D.P. Siddons, B. W. Batterman and J. B. Hastings. *Phys. Rev.* **B50(9)**, 5957 (1994).
6. M. Seto, Y. Yoda, S. Kikuta, X. W. Zhang and M. Ando. *Phys. Rev. Lett.* **74**, 3828 (1995).
7. W. Sturhahn, T. S. Toellner, E. E. Alp, X. W. Zhang, M. Ando, Y. Yoda, S. Kikuta, M. Seto, C. W. Kimball and B. Dabrovsky. *Phys. Rev. Lett.* **74**, 3832 (1995).
8. A. I. Chumakov, R. Rüffer, A. Q. R. Baron, H. Grünsteudel and H. F. Grünsteudel. *Phys. Rev.* **B54**, 9596 (1996).
9. H. Grünsteudel, A. I. Chumakov, H. F. Grünsteudel, A. Q. R. Baron, R. Rüffer, A. X. Trautwein, H. Winkler, and H. Toftlund. In *Proceedings of the International Conference on Bioinorganic Chemistry.* Yokohama, Japan, August 1997.
10. H. Grünsteudel, H. Paulsen, W. Meyer-Klaucke, H. Winkler, A. X. Trautwein, H. F. Grünsteudel, A. Q.R. Baron, A. I. Chumakov, R. Rüffer and H. Toftlund. In *Proceedings of the International Conference on the Applications of the Mössbauer Effect.* Rio de Janeiro, Brazil, September 1997.
11. O. Leupold, E. Gerdau, D. Giesenberg, J. Metge, K. Quast, H. D. Rüter, S. Schwendy, H. Grünsteudel, W. Meyer-Klaucke, A. X. Trautwein, H. Winkler, H. F. Grünsteudel, and R. Rüffer. In *HASYLAB Annual Report*, p. 975. Hamburg (1994).
12. T. Ishikawa, Y. Yoda, K. Izumi, C. K. Suzuki, X. W. Zhang, M. Ando and S. Kikuta. *Rev. Sci. Instr.* **63**, 1015 (1992).
13. T. S. Toellner, T. Mooney, S. Shastri and E. E. Alp. *Proc. SPIE* **1740**, 218 (1992).
14. A. Q. R. Baron, and S. L. Ruby. *Nucl. Instr. Meth.* **A 343**, 517 (1994).
15. J. P. Hannon and G. T. Trammell. In *Resonant Anomalous X-Ray Scattering, Theory and Applications*, p. 565. G. Materlik, C. J. Sparks and K. Fischer (Eds.). Elsevier, N. Y. (1994).
16. Yu. Kagan, A.M. Afanas'ev and V. G. Kohn. *J. Phys. C: Solid State Physics* **12**, 615 (1979).
17. W. Sturhahn and E. Gerdau. *Phys. Rev.* **B49**, 9285 (1994).
18. O. Leupold, H. Grünsteudel, W. Meyer-Klaucke, H. F. Grünsteudel, H. Winkler, D. Mandon, H. D. Rüter, J. Metge, E. Realo, E. Gerdau, A. X. Trautwein and R. Weiss. In *Conference Proceedings "ICAME 95"*, p. 857. I. Ortalli (Ed.). SIF, Bologna (1996).
19. M. Schappacher, L. Ricard, J. Fischer, R. Weiss, E. Bill, R. Montiel-Montoya, H. Winkler and A. X. Trautwein. *Eur. J. Biochem.* **168**, 419 (1987).
20. H. Winkler, W. Meyer-Klaucke, S. Schwendy, A. X. Trautwein, B. F. Matzanke, O. Leupold, H. D. Rüter, M. Haas, E. Realo, D. Mandon and R. Weiss. In *Proceedings of the International Conference on the Applications of the Mössbauer Effect.* Rio de Janeiro, Brazil, September 1997.
21. M. Haas, E. Realo, H. Winkler, W. Meyer-Klaucke, A. X. Trautwein, O. Leupold and H. D. Rüter. *Phys. Rev.* B (in press).
22. A. X. Trautwein, E. Bill, E. L. Bominaar and H. Winkler. *Struct. and Bond.* **78**, 1 (1991).
23. E. L. Bominaar, X.-Q. Ding, A. Gismelseed, E. Bill, H. Winkler, A. X. Trautwein, H. Nasri, J. Fischer and R. Weiss. *Inorg. Chem.* **31**, 1845 (1992).